

ORIGINAL PAPER

Yoshihiro Kawakami · Hiromasa Ikuta
Masataka Wakihara

Ionic conduction of lithium for Perovskite-type compounds, $\text{Li}_x\text{La}_{(1-x)/3}\text{NbO}_3$ and $(\text{Li}_{0.25}\text{La}_{0.25})_{1-x}\text{Sr}_{0.5x}\text{NbO}_3$

Received: 12 September 1997 / Accepted: 15 November 1997

Abstract Perovskite-type compounds, $\text{Li}_x\text{La}_{(1-x)/3}\text{NbO}_3$ and $(\text{Li}_{0.25}\text{La}_{0.25})_{1-x}\text{Sr}_{0.5x}\text{NbO}_3$ as lithium ionic conductors, were synthesized by a solid-state reaction. From powder X-ray diffraction, the solid solution ranges of the two compounds were determined to be $0 \leq x \leq 0.25$ and $0 \leq x \leq 0.125$, respectively. In the $\text{Li}_x\text{La}_{(1-x)/3}\text{NbO}_3$ system, the ionic conductivity of lithium at room temperature, σ_{25} , exhibited a maximum value of $4.7 \times 10^{-5} \text{ S} \cdot \text{cm}^{-1}$ at $x = 0.10$. However, because of the decrease in the lattice parameters with increasing Li concentration x , σ_{25} of the samples decreased with increasing x from 0.10 to 0.25. Also, in the $(\text{Li}_{0.25}\text{La}_{0.25})_{1-x}\text{Sr}_{0.5x}\text{NbO}_3$ system, the lattice parameter increased with the increase of Sr concentration and the σ_{25} achieved a maximum ($7.3 \times 10^{-5} \text{ S} \cdot \text{cm}^{-1}$ at 25 °C) at $x = 0.125$.

Key words Lithium ionic conductor · Perovskite-type compound · Lithium lanthanum niobate · Lithium lanthanum strontium niobate · Ionic conductivity

Introduction

In recent years, lithium secondary batteries have been developed for the power sources of electronic devices because of their high energy density and high discharge voltage. In almost all the researches on lithium secondary batteries, organic electrolytes have been used. However, the use of organic electrolytes may cause many technological problems, e.g. leakage, combustibility and electrochemical decomposition at relatively low charge voltage. To overcome these problems, all-solid batteries in which an inorganic solid electrolyte is substituted for the liquid electrolyte have attracted much attention [1]. However, all a few solid lithium secondary

batteries have been commercialized in earnest because of lower electrical conductivity and poor chemical stability of the solid electrolytes.

In spite of such difficult circumstances, there have recently been several reports on perovskite oxides containing rare earth metals and lithium, which has a high ionic conductivity. In particular, Inaguma et al. [2–4] and Belous et al. [5] have reported that lanthanum lithium titanates with the perovskite structure exhibit very high ionic conductivity ($\sim 10^{-3} \text{ S} \cdot \text{cm}^{-1}$) at room temperature. Also, Latie et al. [6] have investigated the ionic conduction of lithium in the $\text{Li}_x\text{Ln}_{1/3}\text{Nb}_{1-x}\text{Ti}_x\text{O}_3$ ($\text{Ln} = \text{La}, \text{Nd}$) system with a $\text{Ln}_{1/3}\text{NbO}_3$ perovskite-type structure. Such a high lithium ionic conductivity of these perovskite compounds is considered to come from the presence of a vacancy on the A site and a large number of equivalent sites for the lithium ion (Li^+) to move freely in the A site space of the perovskites.

The perovskite compound $\text{La}_{1/3}\text{NbO}_3$ has a unique structure (space group: $\text{Pmmm}[7]$). The NbO_3 framework is made up of NbO_6 octahedra sharing common corners in three space directions. The unit cell of $\text{La}_{1/3}\text{NbO}_3$ contains two NbO_6 octahedra, while 2/3 of 1a sites ($z = 0$) are occupied by La atoms and 1c sites ($z = 1/2$) are unoccupied (Fig. 1). Such a distribution leads to twice the a -parameter of the cubic perovskite-type cell, so that tetragonal symmetry could be expected ($a_{\text{tetra}} \approx a_{\text{cub}}$, $c_{\text{tetra}} \approx 2a_{\text{cub}}$). In fact, the crystal has orthorhombic symmetry because a small orthorhombic distortion occurs [6, 7].

Belous et al. [8, 9] have prepared the perovskite compound $\text{La}_{2/3-x}\text{Li}_{3x}\text{Nb}_2\text{O}_6$ (by substitution of Li^+ for part of the La^{3+} in $\text{La}_{2/3}\text{Nb}_2\text{O}_6$) with this unique structure and investigated the crystal structure and ionic conductivity of the lithium.

In the present study, we have also investigated both the lithium ionic conduction and the crystal structure of the perovskite compound $\text{Li}_x\text{La}_{(1-x)/3}\text{NbO}_3$ and have found that this perovskite compound shows high ionic conductivity at room temperature. Also, in order to expand the lattice of this perovskite, we have prepared

Y. Kawakami (✉) · H. Ikuta · M. Wakihara
Department of Chemical Engineering, Faculty of Engineering,
Tokyo Institute of Technology, 2-12-1 O-okayama,
Meguro, Tokyo 152, Japan Tel.: +81-3-5734 3037;
Fax: +81-3-5734 2146; e-mail: mwakihar@o.cc.titech.ac.jp

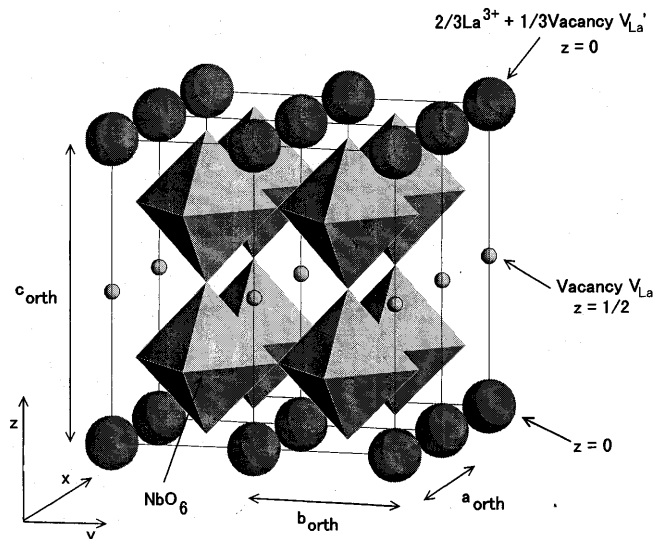


Fig. 1 The structure of $\text{La}_{1/3}\text{NbO}_3$

the perovskite compounds $(\text{Li}_{0.25}\text{La}_{0.25})_{1-x}\text{Sr}_{0.5x}\text{NbO}_3$ by substitution of the larger Sr^{2+} for part of equal amounts of the smaller Li^+ and La^{3+} in $\text{Li}_{0.25}\text{La}_{0.25}\text{NbO}_3$ and have attempted to improve the ionic conduction of lithium by this expansion of the lattice.

Experimental

Samples were prepared by a conventional solid-state reaction. Li_2CO_3 (99.9%, Soekawa Chemical Co.), SrCO_3 (99.9%, Soekawa Chemical Co.), La_2O_3 (99.9%, Soekawa Chemical Co.) and Nb_2O_5 (99.9%, Soekawa Chemical Co.) were used as starting materials. These reagents in the desired ratio were mixed in an agate mortar with ethanol. A mixture of starting materials was pelletized and heated at 800°C for 2 h and then at 1100°C – 1250°C for 24 h in air with several intermediate grindings. X-ray diffraction patterns of the powdered samples were obtained using an X-ray diffractometer (Rigaku: RINT 2500V) equipped with a curved graphite monochromator. The lattice parameters were evaluated under the experimental conditions, 40 kV and 150 mA.

Ionic conductivity for the bulk of the sample was measured by the a.c. impedance technique. The pelletized sample was sintered at 1200 – 1250°C for 24 h. After polishing both sides of the pellet with an emery paper (No. 1200), the pellet was washed in acetone using an ultrasonic cleaner and dried at 110°C in a vacuum. The size of the pellet was about 5 mm in diameter and about 2 mm in thickness. Gold was sputtered on both sides of the pellet surface in order to maintain the ohmic contact of the electrodes. Complex impedance was measured using an LF impedance analyzer 4192A(HP) under vacuum over the temperature range 20 – 300°C and over the frequency range 5 – 1.3×10^7 Hz. The electronic conductivity was measured by the d.c. polarization method.

Results and discussion

$\text{Li}_x\text{La}_{(1-x)/3}\text{NbO}_3$ system

Figure 2a shows the powder X-ray diffraction patterns of the $\text{Li}_x\text{La}_{(1-x)/3}\text{NbO}_3$ system ($x = 0, 0.10, 0.20, 0.25$ and 0.30). The only perovskite phase was observed in the composition range from $x = 0$ to $x = 0.25$, while a small

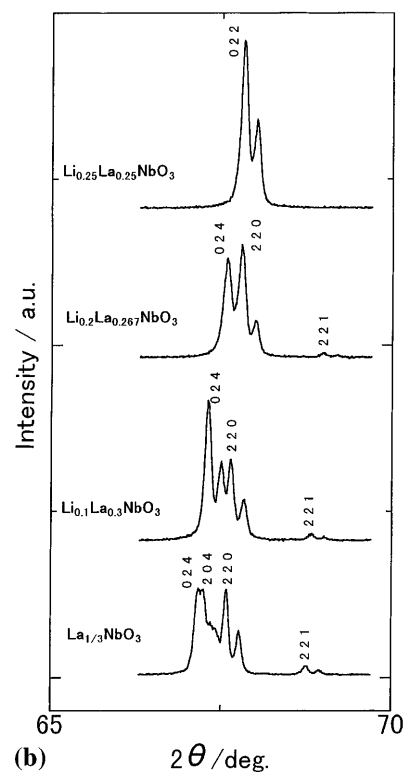
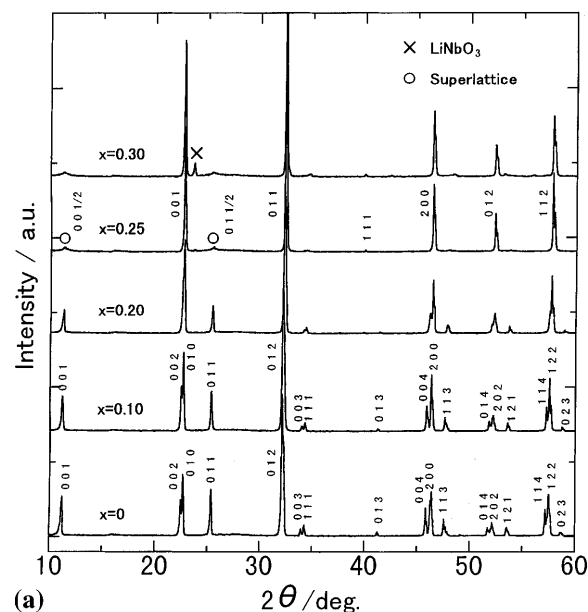


Fig. 2a Powder X-ray diffraction patterns of $\text{Li}_x\text{La}_{(1-x)/3}\text{NbO}_3$ samples with $x = 0, 0.10, 0.20, 0.25$ and 0.30 , and b Variation of the powder X-ray diffraction patterns with Li fraction x in $\text{Li}_x\text{La}_{(1-x)/3}\text{NbO}_3$

amount of LiNbO_3 phase with ilmenite-type structure was observed in the sample at $x = 0.30$. Therefore, the homogeneous region of the $\text{Li}_x\text{La}_{(1-x)/3}\text{NbO}_3$ system with the perovskite structure was determined to be $0 \leq x \leq 0.25$.

Belous et al. [8] have reported that the crystal symmetry changed from orthorhombic to tetragonal and

then to cubic with increasing Li fraction x . In this study, the X-ray diffraction patterns of the samples with $x \leq 0.05$ were also indexed in an orthorhombic system because the (024) peak in tetragonal split into two peaks (024) and (204) in orthorhombic (Fig. 2b). Furthermore, when Li fraction x became $x \geq 0.10$, as shown in Fig. 2b, overlap of the (204) line and the (024) line in the orthorhombic system was observed. This indicates that the lattice parameter a_{orth} becomes equal to b_{orth} in the orthorhombic cell at $x = 0.10$, with a transformation from orthorhombic to tetragonal. Therefore, the X-ray diffraction patterns of the samples with $0.10 \leq x \leq 0.20$ were indexed in the tetragonal system. Also, when the Li fraction was $x = 0.25$, the (024) line and the (220) line in the tetragonal system overlapped with each other (Fig. 2b), and the (001) line and the (011) line (Fig. 2a) in the tetragonal system became broad and weak in intensity. This indicated that the ordered distribution of La^{3+} ions shown in Fig. 1 is destroyed, and that the La^{3+} ions, Li^+ ions and vacancies almost randomly occupy 12-coordinated sites (A sites) among the NbO_6 network, and the lattice parameter c_{tetra} becomes equal to $2 \times a_{\text{tetra}}$ in the tetragonal cell because of the stacking of two perovskite-cubic cells. Therefore, it is considered that the sample with $x = 0.25$ has a cubic-like structure, namely, the pseudo-cubic structure. However, because broad and weak-intensity peaks were observed in the X-ray diffraction pattern at $x = 0.25$, as shown by open circles in Fig. 2a, which could be produced by a superlattice with twice the cubic lattice parameter along c -axis, it seems that two planes which have slightly different occupancy of La^{3+} ions in each would exist, and these two planes would be ordered alternately perpendicular to the c -axis. The variation of the lattice parameters with Li fraction x is shown in Fig. 3. The lattice parameters decreased with increasing Li fraction x , and especially a marked decrease in the lattice parameter c was observed. Probably, the perovskite cell would shrink because the electrostatic interaction in-

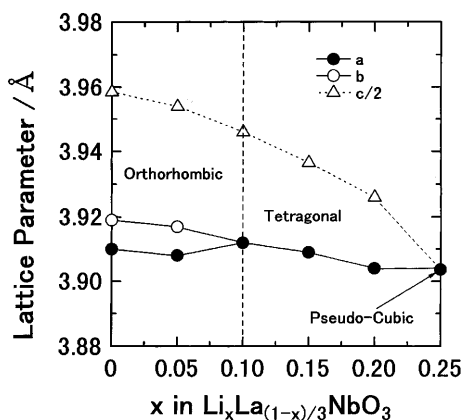


Fig. 3 Variation of the lattice parameters with Li fraction x in $\text{Li}_x\text{La}_{(1-x)/3}\text{NbO}_3$

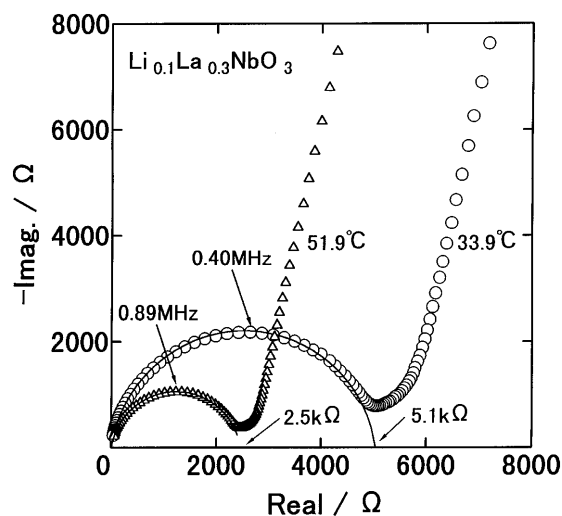


Fig. 4 Typical example of the Cole-Cole plots for the sample ($\text{Li}_{0.1}\text{La}_{0.3}\text{NbO}_3$)

creased along the c -axis because of the introduction of Li^+ ions into V_{La} sites ($z = 1/2$).

Figure 4 shows the Cole-Cole plots of $\text{Li}_{0.1}\text{La}_{0.3}\text{NbO}_3$ obtained from a.c. impedance measurement. The bulk resistance of the sample was estimated from the crossing point of the extrapolated semicircle with the real axis at lower frequency range. Figure 5 shows the reciprocal temperature dependence of ionic conductivity for the sample with lithium fraction x in $0.05 \leq x \leq 0.25$ (Arrhenius plots). All the profiles exhibited an almost linear relationship. Since the electronic conductivity of all the samples was estimated to be of the order of 10^{-10} – $10^{-9} \text{ S} \cdot \text{cm}^{-1}$ at room temperature, the electrical conduction of the sample might be almost ionic.

The variation in ionic conductivity at room temperature, σ_{25} , and the activation energy E_a for ionic

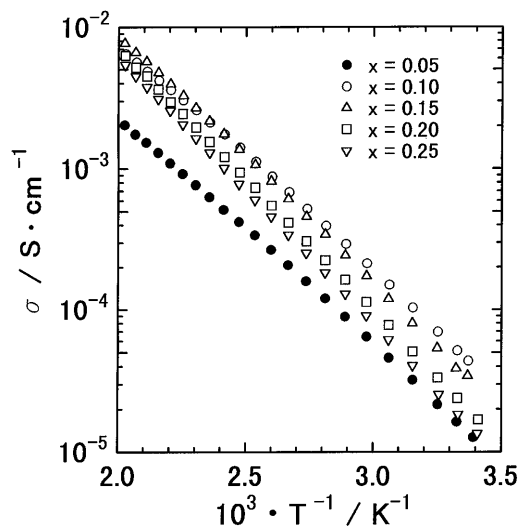


Fig. 5 Typical Arrhenius plots of the ionic conductivity for $\text{Li}_x\text{La}_{(1-x)/3}\text{NbO}_3$ samples with $x = 0.05, 0.10, 0.15, 0.20$ and 0.25

conduction with Li fraction x are shown in Fig. 6. The value of σ_{25} exhibited a maximum ($4.7 \times 10^{-5} \text{ S} \cdot \text{cm}^{-1}$) at $x = 0.10$, while the activation energy E_a monotonously increased with increasing Li fraction x .

Inaguma et al. [3] have considered the variation of ionic conductivity for lanthanum lithium titanate using the relationship between Li fraction and A site vacancy. The ionic conductivity σ is ordinarily given as follows:

$$\sigma = |e| \cdot n \cdot \mu \quad (1)$$

where $|e|$ is the charge of Li^+ , n is the density of Li^+ and μ is the mobility of Li^+ . According to the electric neutrality condition in $(\text{Li}_x\text{La}_{(1-x)/3}\square_{2(1-x)/3})\text{NbO}_3$, the fractions of Li^+ , La^{3+} and vacancies in the A sites are x , $(1-x)/3$ and $2(1-x)/3$, respectively. Since it is expected that Li^+ can migrate only through the vacant A sites, and its mobility μ is proportional to the fraction of vacancy, so the ionic conductivity in Eq. 1 is proportional to the following factor

$$\sigma = |e| \cdot n \cdot \mu \propto x \cdot \frac{2}{3} \cdot (1-x) = -\frac{2}{3} \cdot \left(x - \frac{1}{2}\right)^2 + \frac{1}{6} \quad (2)$$

Equation 2 indicates that σ increases until $x = 0.5$. However, in this study, σ_{25} achieved a maximum value at $x = 0.10$ and decreased over the range from $x = 0.10$ to $x = 0.25$. This suggests that the mobility μ depends not only on the fraction of vacancy but also on the lattice parameters. In this study, the activation energy increased with increasing Li fraction x according to the shrinkage of the lattice. The mobility μ would decrease considerably with increasing Li fraction x because of this increase in the activation energy. Consequently, in spite of the increase in the density of Li n with increasing Li fraction x , the σ_{25} value would begin to decrease from $x = 0.10$ because the mobility μ decreases considerably.

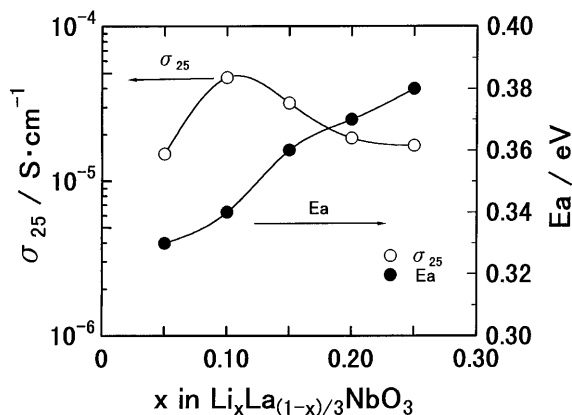


Fig. 6 Variations of the ionic conductivity at room temperature, σ_{25} , (open circles) and the activation energy E_a for ionic conduction (closed circles) with Li fraction x in $\text{Li}_x\text{La}_{(1-x)/3}\text{NbO}_3$

The $(\text{Li}_{0.25}\text{La}_{0.25})_{1-x}\text{Sr}_{0.5x}\text{NbO}_3$ system

In order to improve the ionic conductivity of $\text{Li}_x\text{La}_{(1-x)/3}\text{NbO}_3$, it would be necessary to expand the lattice of perovskite. The substitution of the larger Sr^{2+} (1.44 Å) for the smaller La^{3+} (1.36 Å) and Li^+ (0.92 Å [10]) in $\text{Li}_{0.25}\text{La}_{0.25}\text{NbO}_3$ with the maximum Li fraction may contribute to the expansion of the lattice of the perovskite for improving the ionic conductivity.

Figure 7 shows the powder X-ray diffraction patterns of the $(\text{Li}_{0.25}\text{La}_{0.25})_{1-x}\text{Sr}_{0.5x}\text{NbO}_3$ system ($x = 0, 0.05, 0.125$ and 0.150). The only cubic perovskite phase of the $(\text{Li}_{0.25}\text{La}_{0.25})_{1-x}\text{Sr}_{0.5x}\text{NbO}_3$ system was observed in the composition range from $x = 0$ to $x = 0.125$, while a small amount of SrNb_2O_6 phase was observed in the sample with $x = 0.15$. Therefore, the homogeneous region of the $(\text{Li}_{0.25}\text{La}_{0.25})_{1-x}\text{Sr}_{0.5x}\text{NbO}_3$ system with the cubic perovskite structure was determined to be in the range $0 \leq x \leq 0.125$. The lattice parameter of the cubic phase increased with increasing Sr fraction x (Fig. 8). This indicates that the lattice of the sample expands because of the substitution of the larger Sr^{2+} for the smaller La^{3+} and Li^+ in A sites.

Figure 9 shows the variations of ionic conductivity at room temperature, σ_{25} , and the activation energy E_a with the increase of Sr fraction x . In spite of the decrease in the amount of Li^+ ions due to the substitution of Sr^{2+} for La^{3+} and Li^+ , the ionic conductivity at room temperature, σ_{25} , increased with increasing Sr fraction x and achieved a maximum ($7.3 \times 10^{-5} \text{ S} \cdot \text{cm}^{-1}$ at 25°C) at the end composition $x = 0.125$, while the activation energy for ionic conduction decreased with increasing x . Allowing for the fraction of vacancy in A site being always constant, this indicates that the mobility of Li^+

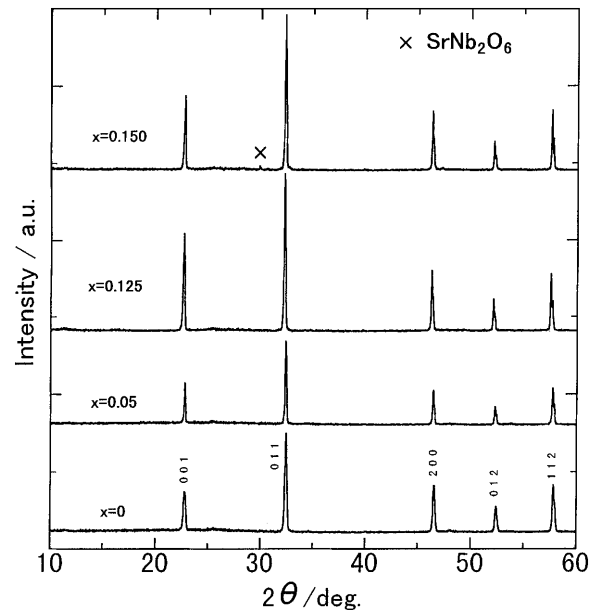


Fig. 7 Powder X-ray diffraction patterns of $(\text{Li}_{0.25}\text{La}_{0.25})_{1-x}\text{Sr}_{0.5x}\text{NbO}_3$ samples ($x = 0, 0.05, 0.125$ and 0.150)

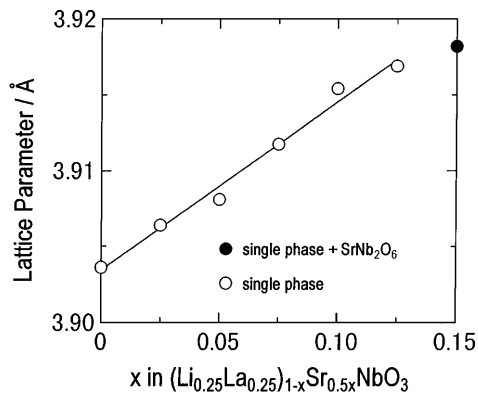


Fig. 8 Variation of the lattice parameter with Sr fraction x in $(\text{Li}_{0.25}\text{La}_{0.25})_{1-x}\text{Sr}_{0.5x}\text{NbO}_3$

ions would increase accompanying the increase in σ_{25} because of the expansion of the lattice by the substitution of Sr^{2+} for Li^+ and La^{3+} .

Conclusions

In the present study, the perovskite compounds $\text{Li}_x\text{La}_{(1-x)/3}\text{NbO}_3$ and $(\text{Li}_{0.25}\text{La}_{0.25})_{1-x}\text{Sr}_{0.5x}\text{NbO}_3$ were synthesized by a solid-state reaction. The homogeneous region of the $\text{Li}_x\text{La}_{(1-x)/3}\text{NbO}_3$ system was determined to be in the range $0 \leq x \leq 0.25$. The crystal symmetry changed from orthorhombic to tetragonal and then pseudo-cubic with increasing Li fraction x . Also, the lattice parameters decreased with the increase of Li fraction x . The activation energy E_a monotonously increased with increasing x , while σ_{25} exhibited a maximum ($4.7 \times 10^{-5} \text{ S} \cdot \text{cm}^{-1}$ at 25°C) at $x = 0.10$.

In the $(\text{Li}_{0.25}\text{La}_{0.25})_{1-x}\text{Sr}_{0.5x}\text{NbO}_3$ system, the homogeneous region was determined to be in the range $0 \leq x \leq 0.125$. The cubic lattice parameter increased with increase of Sr fraction. The σ_{25} value increased with increasing Sr fraction x and achieved a maximum ($7.3 \times 10^{-5} \text{ S} \cdot \text{cm}^{-1}$ at 25°C) at $x = 0.125$, while the activation energy E_a decreased with increasing x . This indicates that the ionic conduction becomes easier by expansion of the perovskite lattice due to the substitution of Sr^{2+} for La^{3+} and Li^+ . It has been found that

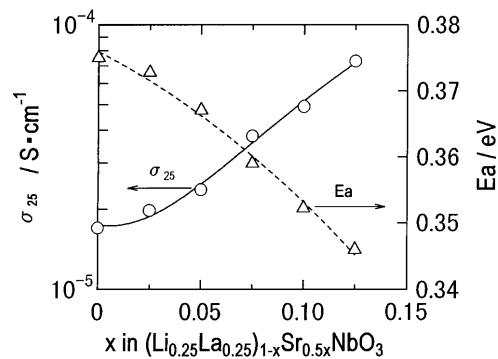


Fig. 9 Variations of the ionic conductivity at room temperature, σ_{25} , (open circles) and the activation energy E_a for ionic conduction (triangle) with Sr fraction x in $(\text{Li}_{0.25}\text{La}_{0.25})_{1-x}\text{Sr}_{0.5x}\text{NbO}_3$

the substitution of the larger Sr^{2+} for the smaller La^{3+} and Li^+ is a more effective method for improving ionic conduction.

Acknowledgements The authors are grateful to Dr. M. Itoh and Dr. Y. Inaguma of Tokyo Institute of Technology for useful discussions. Support from the Grant-in-Aid for Scientific Research in Priority area No.08220220 from the Ministry of Education, Science and Culture is also acknowledged.

References

1. Kanehori K, Matumoto K, Miyauchi K, Kudo T (1983) *Solid State Ionics* 9/10: 1445
2. Inaguma Y, Chen L, Itoh M, Nakamura T, Uchida T, Ikuta H, Wakihara M (1993) *Solid State Commun* 86: 689
3. Inaguma Y, Chen L, Itoh M, Nakamura T (1994) *Solid State Ionics* 70/71: 196
4. Itoh M, Inaguma Y, Jung WH, Chen L, Nakamura T (1994) *Solid State Ionics* 70/71: 203
5. Belous AG, Novitskaya GN, Polyanetskaya SV, Gornikov Yu I (1987) *Izv.Akad.Nauk SSSR, Neorg Mater*: 470
6. Latie L, Villeneuve G, Conte D, Le Felm G (1984) *J Solid State Chem* 51: 293
7. Nadiri A, Le Felm G, Delmas C (1988) *J Solid State Chem* 73: 338
8. Belous AG, Didukh IR, Novosadova EB, Pashkova EV, Khomenko BS (1990) *Izv Akad Nauk SSSR, Neorg Mater* 26: 1294
9. Belous AG (1996) *Solid State Ionics* 90: 193
10. Shannon RD (1976) *Acta Cryst A*32: 751